



Quantum confinement of Mott electrons in ultrathin LaNiO₃/LaAlO₃ superlattices

Jian Liu,^{1,2,*} S. Okamoto,³ M. van Veenendaal,^{4,5} M. Kareev,¹ B. Gray,¹ P. Ryan,⁴ J. W. Freeland,⁴ and J. Chakhalian¹

¹*Department of Physics, University of Arkansas, Fayetteville, Arkansas 72701, USA*

²*Advanced Light Source, Lawrence Berkeley National Laboratory, Berkeley, California 94720, USA*

³*Materials Science and Technology Division, Oak Ridge National Laboratory, Oak Ridge, Tennessee 37831, USA*

⁴*Advanced Photon Source, Argonne National Laboratory, Argonne, Illinois 60439, USA*

⁵*Department of Physics, Northern Illinois University, DeKalb, Illinois 60115, USA*

(Received 26 January 2011; published 13 April 2011)

We investigate the electronic reconstruction in (LaNiO₃)_n/(LaAlO₃)₃ ($n = 3, 5$, and 10) superlattices due to the quantum confinement (QC) by dc transport and resonant soft x-ray absorption spectroscopy. In proximity to the QC limit, a Mott-type transition from an itinerant electron behavior to a localized state is observed. The system exhibits tendency toward charge-order during the transition. *Ab initio* cluster calculations are in good agreement with the absorption spectra, indicating that the apical ligand hole density is highly suppressed, resulting in a strong modification of the electronic structure. At the dimensional crossover cellular dynamical-mean-field calculations support the emergence of a Mott insulator ground state in the heterostructured ultrathin slab of LaNiO₃.

DOI: [10.1103/PhysRevB.83.161102](https://doi.org/10.1103/PhysRevB.83.161102)

PACS number(s): 73.21.-b, 78.70.Dm

Prompted by the discovery of high- T_c superconductivity in cuprate compounds there has been a surge of activity to discover materials with even higher transition temperature.¹ Recent remarkable advances in synthesis of artificial layers of complex oxides along with the progress in computational methods have reenergized the search for novel superconductors outside of the cuprate family.^{2,3}

Toward the challenge, a recent proposal has been put forward to use heterostructuring and orbital engineering to turn hole-doped alternating unit-cell thin layers of a correlated metal, LaNiO₃ (LNO), and a band-gap dielectric, LaAlO₃ (LAO).⁴ The proposal utilizes the Ni^{III} $3d^7$ low-spin state in the bulk with a single unpaired electron occupying the degenerate ($d_{x^2-y^2}/d_{3z^2-r^2}$) e_g orbital whose nodes point to the planar and apical ligands of the octahedra, respectively. Both t - J and LDA + DMFT calculations^{4,5} suggest that the quantum confinement together with the electronic correlations should make it possible to localize or empty the $d_{3z^2-r^2}$ band leaving the conduction electron in the $d_{x^2-y^2}$ band. Epitaxial strain is also suggested as a means of the orbital control to manipulate the $d_{3z^2-r^2}$ orbital to appear above $d_{x^2-y^2}$ and play the analogous role of the axial orbital of the high- T_c cuprates.

Despite the attractive simplicity of the structure, the experimental realization of a LNO/LAO superlattice (SL) presents a large degree of ambiguity in selecting a specific electronic ground state caused by (i) the intrinsic propensity of ortho-nickelates to charge ordering,⁶⁻⁸ (ii) orbital polarization due to chemical confinement imposed by interfacial bonding,^{9,10} (iii) polar discontinuity,^{11,12} (iv) epitaxial constraint on the crystal symmetry,^{13,14} and (v) quantum confinement.^{15,16} Even for the undoped LNO/LAO SL (i.e., the proposed parent cupratelike compound), the synergetic action of these phenomena will likely render the theoretical problem intractable to *a priori* predict whether the cupratelike physics can be experimentally realized.

Here we report on emergence of a Mott-type metal-insulator transition (MIT) at the dimensional crossover in the experimentally realized (LNO)_n/(LAO)₃ SLs. By using transport measurement and soft x-ray absorption spectroscopy in combination with cluster calculations and cellular

dynamical-mean-field theory calculations, we demonstrate the presence of a charge-localized ground state at the quantum confinement limit caused by strongly enhanced correlations and broken translational symmetry across the interface. In sharp contrast to conventional bandwidth control, the observed MIT is a continuous one with a critical region due to an emerging correlated gap imposed by confined dimensionality. The system also exhibits a tendency toward charge ordering as a competing state during the transition. Microscopically, the crossover from the localized to itinerant behaviors is driven by a strong competition between the reduced covalency of the Ni-O-Al bond and the recovery of the ligand hole density within the LNO slab.

High-quality epitaxial [(LNO)_n/(LAO)₃]_N SLs ($n = 3, 5$, and 10 with $N = 10, 4$, and 2 , respectively) were grown by laser molecular beam epitaxy with *in situ* monitoring by reflection high-energy electron diffraction, as described in Refs. 17 and 12; +2.2% tensile strain is applied with TiO₂-terminated (001) SrTiO₃ substrates.¹⁸ Atomic force microscopy imaging reveals that the substrate surface morphology is well maintained after the growth; symmetric scans and reciprocal space mapping by synchrotron-based x-ray diffraction indicate coherently grown single crystal heterostructures with the fully strained state.¹⁷

To explicate the evolution of the ground state due to quantum confinement, dc transport measurements from 400 to 2 K were performed in the *van der Pauw* geometry with a commercial physical properties measurement system (PPMS, Quantum Design). The obtained temperature dependent conductivity, $\sigma(T)$, of the SL series is shown in Fig. 1(a). A transition from metallic to insulating behavior can be clearly seen with decreasing n . The inset of Fig. 1(a) also demonstrates orders of magnitude change in σ across the series taken at 10 K. As seen, in analogy to the bulk LNO, the $n = 10$ SL exhibits a highly metallic behavior ascribed to the three-dimensional regime. On the other hand, unlike the bulk, which is known to follow a $T^{3/2}$ dependence at room temperature and switch to a low-temperature T^2 Fermi liquid behavior,¹⁹ the resistivity ρ at $n = 10$ switches from a T -linear behavior above 200 K to a $T^{3/2}$ power law [see Fig. 1(b)].

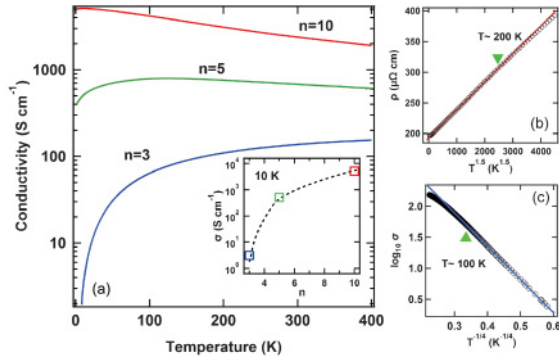


FIG. 1. (Color online) (a) Conductivity of $(\text{LNO})_n/(\text{LAO})_3$ SLs versus temperature. Inset: Conductivity versus n at 10 K. The dashed line is a guide for the eye. (b) Resistivity (circle) as a function of $T^{1.5}$ at $n = 10$. The red (dark gray) solid line is a guide for the eye. (c) $d \log_{10} \sigma$ (circle) as a function of $1/T^{1/4}$ for the $n = 3$ SL shows the low-temperature three-dimensional variable-range hopping behavior. The blue (dark gray) solid line is a guide for the eye.

Note that, while a T -linear dependence was also found in the high-temperature metallic phase of other members of the bulk RENiO_3 ($\text{RE} = \text{rare earth}$) family who have a charge-ordered insulating ground state,²⁰ the low-temperature $T^{3/2}$ behavior of Fermi liquid electrons has been attributed to scattering by bond-length fluctuations due to proximity to a Mott-type MIT from the itinerant side.²¹ These phenomena indicate enhanced electronic correlations in the quantum confinement regime and stronger vibronic fluctuations associated with charge ordering.

The intermediate thickness $n = 5$ SL still shows a clear metallic behavior at high temperatures but reaches a conductivity maximum at $T_{\text{max}} = 120$ K. While the metallicity of LNO films under large tensile strain is known to cease when the thickness is ≤ 3 nm (Ref. 22), it is remarkable that the high-temperature metallic behavior is well maintained in such a thin slab (< 2 nm). This result unambiguously highlights the exquisite role of the confinement structure with interfaces in defining the transport properties of SLs as compared to the bulk LNO and single layer films. Notice, the conductivity σ here is also well below the Ioffe-Regel limit²³ (~ 2000 S/cm), manifesting the modification of the correlation nature of the observed behaviors and the minor role of disorder. Below T_{max} , $\sigma(T_{\text{max}}) - \sigma(2 \text{ K})$ (~ 381.6 S/cm) is as large as $\sigma(2 \text{ K})$ and almost twice $\sigma(T_{\text{max}}) - \sigma(400 \text{ K})$. Neither hopping conductivity nor quantum corrections are found to be able to account for this $d\sigma/dT > 0$ region. This transitional behavior explicitly indicates that all the involved interactions and relevant energy scales, like electron correlations and the bandwidth, are of a similar strength and strongly competing with each other. Thus, $n = 5$ falls into a critical region of the confinement-controlled MIT. Upon entering the insulating phase at $n = 3$, $d\sigma/dT > 0$ at all temperatures and a variable-range hopping behavior is found below 100 K [see Fig. 1(c)], indicating that finite density of states remains within the opening gap during the dimensional crossover.

While transport probes the long-range behavior of the SLs, we carried out detailed soft x-ray absorption measurements to gain microscopic insight into the effect of confinement

on the nature of the MIT. Because of the local core-hole and the element selectivity, resonant x-ray absorption is well suited for investigating the electronic structure of buried layers. All spectra were acquired in the bulk-sensitive fluorescence yield mode at the Ni L -edge at the 4ID-C beamline of the Advanced Photon Source. Precise information on the Ni charge state was obtained by aligning all the spectra to a NiO standard which was measured simultaneously with the SLs. The energy resolution was set at 100 meV. The normalized spectra obtained at 300 K are shown in Figs. 2(a) and 2(b). For direct comparison, the L -edge spectra of bulk LNO and SmNiO_3 (Ref. 24) are included. The partially overlapping $\text{La } M_4$ -edge is subtracted from the Ni L_3 -edge spectra with a Lorentzian function [an example is shown in Fig. 2(c)]. As seen, the energy position and the lineshape of the SLs are close to those of the bulk RENiO_3 ,^{25,26} indicative of a Ni^{II} charge state of the $3d^7$ low-spin configuration. The preservation of the highly unstable Ni^{II} valence state further ensures the absence of the disorder effect. On the other hand, while the multiplet effects are smeared in the metallic bulk LNO, the L_3 -edge spectra of the SL show a pronounced two-peak structure [shaded in green (light gray)], closely resembling the absorption spectrum of the bulk SmNiO_3 [see Fig. 2(a)], which in the bulk is a well-studied case for the charge-ordered ($2\text{Ni}^{II} \rightarrow \text{Ni}^{II} + \text{Ni}^{IV}$) insulating state.^{6,7} As n decreases this multiplet effect becomes more pronounced,

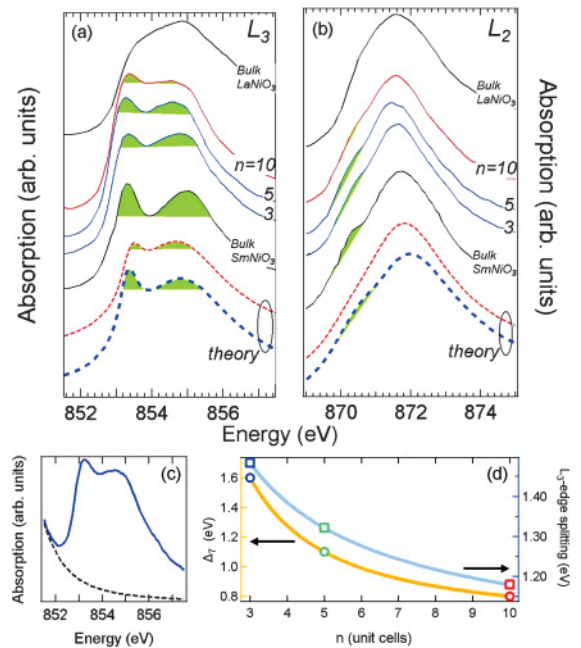


FIG. 2. (Color online) X-ray absorption spectra of $(\text{LNO})_n/(\text{LAO})_3$ SLs at the L_3 -edge (a) and L_2 -edge (b) for $n = 3, 5$, and 10 together with the theoretical calculations (dashed) done for a NiO_6 cluster for a charge-transfer energy of 0.8 (thin red/gray line) and 1.6 (thick blue/gray line) eV. Spectra of bulk LNO and SmNiO_3 ²⁴ are included for comparison. The shaded green (light gray) areas indicate the most significant changes during the evolution. (c) The L_3 -edge spectrum at $n = 5$ (solid) before subtracting the Lorentzian profile (dashed) for the $\text{La } M_4$ -edge. (d) The observed multiplet splitting energy (square) and the corresponding calculated charge-transfer energy (circle) versus n . Solid curves are fits to power law.

particularly in moving from $n = 10$ to 5. The energy separation of the two split peaks is also clearly increasing as shown in Fig. 2(d). The corresponding trend at the L_2 -edge emerges as a developing low-energy shoulder at about 870.5 eV [see Fig. 2(b)]. The observed evolution is reminiscent of that reported for the bulk RENiO_3 when crossing the metal-insulator boundary,²⁶ unambiguously revealing the carrier localization in the presence of a developing correlated gap in the quantum confined LNO slabs and a latent tendency to charge ordering during the three- to two-dimensional crossover. In accordance with the observations from dc transport, the emergence of the multiplet even in the relatively thick LNO slab ($n = 10$) lends solid support to strongly confinement-enhanced correlations. Meanwhile, when subject to this enhancement, the inclination to charge ordering corroborates its role as a primary competing ground state not only in the bulk⁶ but also in the predicted heterostructured LNO.⁴

To shed additional light on the observed spectroscopic results, we performed *ab initio* cluster calculations on a NiO_6 cluster. The model Hamiltonian includes on-site energies, crystal field, Coulomb interaction including the full multiplet structure, and spin-orbit coupling.²⁷ The majority of the parameters are equivalent to those in Ref. 27. The monopole part of the Coulomb interaction is set at 6 eV. The major configurations used in the calculation are $d_{e_g\uparrow}^2 d_{e_g\downarrow}$ and $d_{e_g\uparrow}^2 \underline{L}_{e_g\downarrow}$, where $d_{e_g\sigma}$ and $\underline{L}_{e_g\sigma}$ stand, respectively, for a $3d$ hole and a ligand hole with e_g symmetry and spin $\sigma = \uparrow, \downarrow$. Note that trivalent nickel compounds, such as LNO, are significantly more covalent than divalent systems as the charge-transfer energy $\Delta_n = E(d^{n+1}\underline{L}) - E(d^n)$ decreases due to the change in electron count with $\Delta_7 \cong \Delta_8 - U$, leading to strong mixing between the $d^8\underline{L}$ and d^7 configurations. The degree of Ni-O covalency here is varied by changing the charge-transfer energy Δ_7 . Figure 2(a) shows the result of calculations when Δ_7 was varied from 0.8 to 1.6 eV. The calculation strongly implies that when the local Ni-O covalency is reduced with increasing Δ_7 , the observed evolution of the L_3 -edge multiplet splitting with n is well reproduced. To quantify the n dependence, the value of Δ_7 for each SL is obtained by matching the corresponding size of the splitting. As can be seen in Fig. 2(d), the n dependence of Δ_7 clearly tracks that of the energy separation of the split peaks at the L_3 -edge.

With this excellent agreement between the experimental spectra and the calculation, we can speculate on a possible physical origin of the n dependence of the correlated gap energy. With a decreasing number of LNO slabs, the reducing covalency manifested by the increasing Δ_7 can be connected to the confinement effect which breaks the translation symmetry with interfaces and causes the formation of a significantly less covalent Ni-O-Al chemical bond. This is well in line with the recent density functional theory calculations on similar LNO/LAO SL structures in the two-dimensional limit,^{9,10} demonstrating that the combination of cluster calculation and experimental modulation on dimensionality can be an effective tool for studying heterostructures, even though the cluster model does not explicitly include the interface. The underlying physical picture is that the absence of d -electron states on Al and its much lower electronegativity compared to Ni strongly suppress the ligand hole density on the apical oxygen O_a . Consequently, because of the proximity to the more positively

charged Al ion, the Madelung potential on the interfacial O_a is further raised with respect to the planar O_p ; this leads to further suppression of the apical hole density and charge transfer process. As a result, the interfacial Ni- O_a bond length becomes shorter,⁴ the ligand hole is transferred into the NiO_2 plane and the $d^8\underline{L}$ configuration will acquire more of the $d_{x^2-y^2}$ character. This effect is in close analogy to the physics of cuprates where the Madelung energy of the apical oxygen and the Cu- O_a bond length are believed to be important parameters to control the planar hole density and to stabilize the Zhang-Rice states upon hole doping.²⁸

As discussed before, the cluster calculations can be successfully applied to provide insight into how the local electronic structure is modified in proximity to the interface. However, the observed global MIT resulting from the competition between the short-range electron correlation and the reduced bandwidth subject to quantum confinement is better treated within the layer extension of cellular dynamical-mean-field theory (layer CDMFT)²⁹ with the Lanczos exact diagonalization impurity solver.³⁰ Note that CDMFT was recently applied to explain the opening of a correlation-induced pseudogap in SrVO_3 thin films.³¹ The layer CDMFT we employed here goes beyond that previous study by including short-range correlations within each monolayer to capture the physics of the pseudogap. To make the problem tractable and yet relevant for the SLs we consider the multilayered single-band Hubbard model for Ni $3d$ and simulate the high-energy Al $3s$ states as a vacuum. The short-range correlation is antiferromagnetic as recently suggested in a similar system with the planar $d_{x^2-y^2}$ orbital configuration.⁵ To neutralize the CDMFT's overemphasis on the in-plane correlations, we introduce a small anisotropy between the in-plane t_{in} and the out-of-plane t_{out} transfers as $t_{\text{in}} = t(1 - \delta)$ and $t_{\text{out}} = t(1 + 2\delta)$ so that t_{out} competes with the in-plane correlations. The bandwidth of the bulk noninteracting system is unchanged, $W = 12t$.

Since bulk LNO is a metal we consider moderate values of U/t ($U = 6t$). Figure 3(a) presents the n -dependent evolution of the spectral function. As is clearly seen, the correlation gap in the two-dimensional limit is filled up with density of states and becomes a pseudogap with increasing n , lending theoretical support to the notion that the experimentally observed MIT arises from the dimensional evolution of a quantum confined correlated carriers transforming from an insulator to a metal through a "bad" metal phase. Notice, the sharp quasiparticle

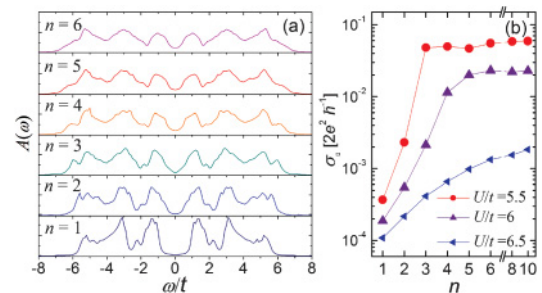


FIG. 3. (Color online) Layer CDMFT results for the multilayer Hubbard model with various thickness n . The transfer anisotropy δ is set at 0.2. (a) Average spectral function for $U/t = 6$. (b) Sheet conductance σ_{\square} versus n for $U/t = 5.5, 6$, and 6.5 .

peak is absent at $\omega = 0$ even in the thickest slab because out-of-plane correlations are treated on a mean-field level. To see the relation between the (pseudo) gap opening and the anomalous transport properties, sheet conductance σ_{\square} is computed by the standard Kubo formula. We introduce an imaginary part $\eta = 0.1t$ to the real frequency ω to represent the finite impurity scattering. As shown in Fig. 3(b), with increasing n , σ_{\square} increases continuously and becomes practically unchanged above a critical thickness n_c below which the pseudogap is pronounced. These results reproduce well the critical regime at $n_c \approx 5$ in the transport measurements and strongly suggest the confinement-controlled short-range electron correlations as the origin of the observed MIT. As discussed earlier, it is known that bulk rare-earth nickelates have an intrinsic propensity toward the charge disproportionation when the electronic bandwidth is reduced.⁷ The result is a complicated three-dimensional ordering of both charge and spin. While such an order might be thought as a complex competing state, we believe that the essential physics of metal-insulator crossover by the quantum confinement is captured by the CDMFT.

In conclusion, we have investigated the quantum confinement effects on the electronic properties of $(\text{LNO})_n/(\text{LAO})_3$ SLs. By lowering the dimensionality of the heterostructured LNO slab, enhanced electron correlations are observed to drive the emergent Mott-type MIT with the latent competing state

of charge ordering. The strong multiplet splitting appearing in x-ray absorption spectra is the effect of the interface leading to the redistribution of ligand hole density and reduction of Ni-O-Al covalency as confirmed by *ab initio* cluster calculations. The result indicates intriguing similarities between the physics of a heterostructured nickelate-based e_g^1 system and parent cuprates. The critical region of the MIT at $n = 5$ deduced from the transport measurements is ascribed to the pseudogap opening due to dimensional crossover and strongly enhanced short-range correlations confirmed by the layer-resolved CDMFT calculations.

The authors acknowledge fruitful discussions with R. Pentcheva, D. Khomskii, A. Millis, and G. A. Sawatzky. J.C. was supported by the DOD-ARO under Grant No. 0402-17291 and the NSF under Grant No. DMR-0747808. Work at the Advanced Photon Source, Argonne, is supported by the US Department of Energy, Office of Science under Grant No. DEAC02-06CH11357. M.v.V. was supported by the US Department of Energy, Office of Basic Energy Sciences, Division of Materials Sciences and Engineering under Contract DE-FG02-03ER46097. S.O. was supported by the Materials Sciences and Engineering Division, Office of Basic Energy Sciences, US Department of Energy.

*jxl026@uark.edu

- ¹J. G. Bednorz, *Nat. Mater.* **6**, 621 (2007).
- ²N. Reyren *et al.*, *Science* **317**, 1196 (2007).
- ³H. Takahashi *et al.*, *Nature (London)* **453**, 376 (2008).
- ⁴J. Chaloupka and G. Khaliullin, *Phys. Rev. Lett.* **100**, 016404 (2008); P. Hansmann, X. Yang, A. Toschi, G. Khaliullin, O. K. Andersen, and K. Held, *ibid.* **103**, 016401 (2009).
- ⁵P. Hansmann, A. Toschi, X. Yang, O. K. Andersen, and K. Held, *Phys. Rev. B* **82**, 235123 (2010).
- ⁶I. I. Mazin, D. I. Khomskii, R. Lengsdorf, J. A. Alonso, W. G. Marshall, R. M. Ibberson, A. Podlesnyak, M. J. Martinez-Lope, and M. M. Abd-Elmeguid, *Phys. Rev. Lett.* **98**, 176406 (2007).
- ⁷G. Catalan, *Phase Transitions* **81**, 729 (2008).
- ⁸M. L. Medarde, *J. Phys.: Condens. Matter* **9**, 1679 (1997).
- ⁹M. J. Han, C. A. Marianetti, and A. J. Millis, *Phys. Rev. B* **82**, 134408 (2010).
- ¹⁰J. W. Freeland, J. Liu, M. Kareev, B. Gray, J. Kim P. Ryan R. Pentcheva, and J. Chakhalian, e-print [arXiv:1008.1518](https://arxiv.org/abs/1008.1518) (to be published).
- ¹¹N. Nakagawa, H. Y. Hwang, and D. A. Muller, *Nat. Mater.* **5**, 204 (2006).
- ¹²Jian Liu *et al.*, *Appl. Phys. Lett.* **96**, 133111 (2010).
- ¹³S. J. May, J. W. Kim, J. M. Rondinelli, E. Karapetrova, N. A. Spaldin, A. Bhattacharya, and P. J. Ryan, *Phys. Rev. B* **82**, 014110 (2010).
- ¹⁴J. Chakhalian, J. M. Rondinelli, J. Liu, B. Gray, M. Kareev, E. Moon, M. Varela, S. G. Altendorf, F. Strigari, B. Dabrowski, L. Tjeng, P. Ryan, and J. Freeland, e-print [arXiv:1008.1373](https://arxiv.org/abs/1008.1373) (to be published).
- ¹⁵S. S. A. Seo *et al.*, *Phys. Rev. Lett.* **104**, 036401 (2010).
- ¹⁶M. Takizawa *et al.*, *Phys. Rev. Lett.* **102**, 236401 (2009).
- ¹⁷M. Kareev, S. Prosandeev, J. Liu, B. Gray, P. Ryan, A. Kareev, E. J. Moon, and J. Chakhalian, e-print [arXiv:1005.0570](https://arxiv.org/abs/1005.0570) (to be published).
- ¹⁸M. Kareev *et al.*, *Appl. Phys. Lett.* **93**, 061909 (2008).
- ¹⁹J.-S. Zhou, J. B. Goodenough, B. Dabrowski, P. W. Klamut, and Z. Bukowski, *Phys. Rev. B* **61**, 4401 (2000); X. Q. Xu, J. L. Peng, Z. Y. Li, H. L. Ju, and R. L. Greene, *ibid.* **48**, 1112 (1993); K. Horiba, R. Eguchi, M. Taguchi, A. Chainani, A. Kikkawa, Y. Senba, H. Ohashi, and S. Shin, *ibid.* **76**, 155104 (2007).
- ²⁰X. Obradors, L. M. Paulius, M. B. Maple, J. B. Torrance, A. I. Nazzari, J. Fontcuberta, and X. Granados, *Phys. Rev. B* **47**, 12353 (1993).
- ²¹F. Rivadulla, J.-S. Zhou, and J. B. Goodenough, *Phys. Rev. B* **67**, 165110 (2003).
- ²²R. Scherwitzl *et al.*, *Appl. Phys. Lett.* **95**, 222114 (2009); J. Son *et al.*, *ibid.* **96**, 062114 (2010).
- ²³N. F. Mott, *Philos. Mag.* **26**, 1015 (1972).
- ²⁴J. W. Freeland *et al.* (unpublished).
- ²⁵M. Medarde, A. Fontaine, J. L. Garcia-Munoz, J. Rodriguez-Carvajal, M. de Santis, M. Sacchi, G. Rossi, and P. Lacorre, *Phys. Rev. B* **46**, 14975 (1992).
- ²⁶C. Piamonteze, F. M. F. de Groot, H. C. N. Tolentino, A. Y. Ramos, N. E. Massa, J. A. Alonso, and M. J. Martinez-Lope, *Phys. Rev. B* **71**, 020406(R) (2005).
- ²⁷M. A. van Veenendaal and G. A. Sawatzky, *Phys. Rev. B* **50**, 11326 (1994).
- ²⁸M. Mori, G. Khaliullin, T. Tohyama, and S. Maekawa, *Phys. Rev. Lett.* **101**, 247003 (2008).
- ²⁹G. Kotliar, S. Y. Savrasov, G. Palsson, and G. Biroli, *Phys. Rev. Lett.* **87**, 186401 (2001).
- ³⁰M. Caffarel and W. Krauth, *Phys. Rev. Lett.* **72**, 1545 (1994).
- ³¹K. Yoshimatsu, T. Okabe, H. Kumigashira, S. Okamoto, S. Aizaki, A. Fujimori, and M. Oshima, *Phys. Rev. Lett.* **104**, 147601 (2010).